Adaptive Distance Protection for Microgrids

Lin, Hengwei; Guerrero, Josep M.; Quintero, Juan Carlos Vasquez; Liu, Chengxi

Published in:
Proceedings of the 41th Annual Conference of IEEE Industrial Electronics Society, IECON 2015

DOI (link to publication from Publisher):
10.1109/IECON.2015.7392185

Publication date:
2015

Document Version
Accepted author manuscript, peer reviewed version

Adaptive Distance Protection for Microgrids

Hengwei Lin[1] Josep M. Guerrero[1] Juan C. Vásquez[1] Chengxi Liu[2]
hwe@et.aau.dk joz@et.aau.dk juq@et.aau.dk chx@energinet.dk
1: Institute of Energy Technology
Aalborg University, 9220 Aalborg East, Denmark
2: Energinet.dk
Tonne Kjærsvej 65, Fredericia, DK-7000, Denmark

***Abstract*—Due to the increasing penetration of distributed generation resources, more and more microgrids can be found in distribution systems. This paper proposes a phasor measurement unit based distance protection strategy for microgrids in distribution system. At the same time, transfer tripping scheme is adopted to accelerate the tripping speed of the relays on the weak lines. The protection methodology is tested on a mid-voltage microgrid network in Aalborg, Denmark. The results show that the adaptive distance protection methodology has good selectivity and sensitivity. What is more, this system also has a good capability on monitoring and control of the network.**

***Index Terms*—Adaptive Distance Protection, Distribution System, Distributed Generation, Distributed Generation, Microgrid, PMU, Reconfiguration, Renewable Energy.**

I. INTRODUCTION

Owing to the rapid growing demand for electricity and significant increase of renewable energy (RE), more and more distributed generation units (DGs) have been installed on the transmission and distribution systems. In Denmark, almost 40% of the installed power has been from RE. It is noticeable that most of the renewable generation is connected to the distribution system, which is below 100kV. For the utility side, integrating large amount of wind power and other forms of localized electricity generation are still the key tasks. However, the increasing penetration of DGs brings challenges to power systems. The protection infrastructure is one of the most important aspects that need to be improved for the modernization of power grid.

Microgrid has been considered as an effective solution to manage the increasing levels of DGs in distribution grid. Due to the increasing integration of DGs in power system, some new challenges should be taken in to account for protection: (1) bidirectional power flow; (2) different fault current level for various operation modes; (3) the randomness and intermittence of RE; (4) looped or meshed network topology. The distribution grids and microgrids are often designed with loops, although they are usually operated in a radial topology. Redundancy is vital to realize high reliability for distribution networks, where the multiple distribution feeders may supply some critical consumers. These loops in the system are disconnected with related switches in normal operation, which can also be intentionally closed to supply some important load when there is a fault on the feeder. At the same time, the installation of DGs in distribution systems brings bidirectional power flow, which may affect the conventional protections designed for single direction. On the other hand, the randomness and intermittence of RE bring uncertainty for the network. These uncertain DGs may influence the fault current level. In the worst cases, the fault may lose their support. Furthermore, some distribution systems with enough electricity supply have the ability to operate in islanded mode, working as a mircogrid, which can lead to the fault current level much lower than in grid-connected mode. This is due to the transmission grid generally has higher short circuit capability compared to the distribution system.

Adaptive overcurrent protection with capabilities time-current discrimination is proposed by some papers to deal with the above problems, which can modify the settings of the relays under different operation modes [1]-[3]. However, the sensitivity of the adaptive overcurrent protection strategies without communication may not meet the requirements in some situations [4]. Conventional distance relay and differential relay are also adopted widely in transmission and distribution system [5]-[10]. Because of the higher selectivity and sensitivity, these two protection strategies have more competitiveness than the time-current based overcurrent protection methodologies for future power system.

Considering the modernization of Danish distribution grid with increasing penetration of RE, this paper proposes an adaptive distance protection with phasor measurement unit (PMU) functions [11] to provide high-resolution real-time measurement. The remainder of this paper is organized as fellows. Section II gives a radial microgrid network in Aalborg, Denmark. The PMU-based dynamic monitoring and control system is proposed for the microgrid in Section III. Section IV introduces the distance protection. A distance protection strategy with transfer tripping for weak lines is presented and tested in Section V. Finally, the conclusion is given in Section VI.

II. MODEL OF THE TEST DISTRIBUTION SYSTEM

Fig.1 gives the test microgrid network. It is a part of the distribution system owned by Distribution System Operator, Himmerlands Elforsyning (HEF) in Aalborg, Denmark. This distribution system contains a combined heat and power (CHP) plant with three 3.3MW gas turbine generators (GTGs) and three small wind farms. Each wind farm consists of two 2WM doubly fed induction generators (DFIG) and one 0.8MW capacitor bank. The configuration of Wind Farm 1 connected on Bus3 is shown in Fig.2. The WTG data are given in Table I. The data of the 3.3MW GTG are list in Table II. The relevant

governor and excitation control models for the generators are integrated in the test. Table III lists the data of the lines.

TABLE I. Wind Turbine Generator Data

Parameters	Value
Rated power (MW)	2
Stator rated voltage (kV)	0.69
Stator resistance (p.u.)	0.0108
Stator reactance (p.u.)	0.0121
Magnetic reactance (p.u.)	3.362
Rotor resistance (p.u.)	0.004
Rotor reactance (p.u.)	0.05
Crowbar resistance (p.u.)	0.5
Crowbar reactance (p.u.)	0.1
Generator inertia (kgm^2)	255.105
Rotor inertia (kgm^2)	$6.1x10^6$
Drive train stiffness (Nms/rad)	$8.3x10^7$
Drive train damping (Nms/rad)	$1.4x10^6$
Nominal turbine speed (rpm)	18
Rotor radius (m)	50
Max. current for crowbar insertion (kA)	5

TABLE II. Gas Turbine Generator Data

Parameters	Value
Rated power (MW)	3.3
Rated voltage (kV)	6.3
Stator resistance (p.u.)	0.0108
Stator reactance (p.u.)	0.0121
d-axis reactance X_d, X_d^I, X_d^{II} (p.u.)	1.5,0.256,0.168
q-axis reactance X_q, X_q^{II} (p.u.)	0.75,0.184
d-axis time constant T_{d0}^I, T_{d0}^{II} (sec)	0.53,0.03
q-axis time constant T_{q0}^{II} (sec)	0.03
Inertia time constant (sec)	0.54

TABLE III. Line Data

line	Resistance (Ohm)	Reactance (Ohm)
Line12	1.24	1.21
Line23	0.372	0.363
Line34	0.992	0.968
Line45	0.928	0.75
Line56	0.2295	0.1875
Line17	0.124	0.121
Line16	1.224	1.0

The maximum and minimum short circuit powers of the transmission grid are 249 MVA and 224 MVA. The test microgrid here can be able to be operated in the islanded mode, supporting all the loads in the network. Load 5 is a critical consumer in the system. The relays represented by "*R*" are shown in Fig.1. The numbers behind "*R*" represent the beginning bus and end bus in the primary protection zone respectively. Normally, the distribution system connects to the transmission grid with Line16 disconnected in the network, working as a radial topology. The connection of the wind farms and CHP are managed by the relays located at each point of common coupling (PCC). The relays in this microgrid are controlled by HEF, such as R30, R40, R60 and R17 in the network. However, the interior protection of the power plant is managed by the property owner.

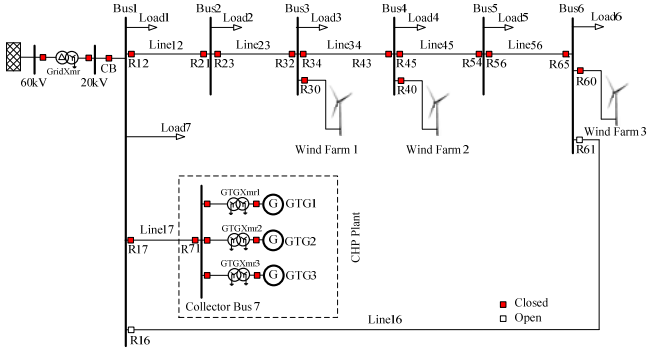

Fig. 1. The test Microgrid network in Aalborg.

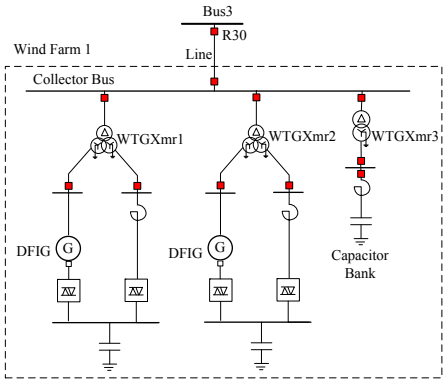

Fig. 2. Wind Farm 1 in the microgrid.

III. Dynamic Monitoring and Control System

PMU is a device that measures the electrical variables adopting a common time source for the synchronization of those measured variables [11]. Synchrophasor measurement function has already been able to be integrated into the modern intelligent electrical devices (IEDs) such as the digital relays, fault recorders and the remote terminal unites in the power plants. In the microgrid, a data concentrator (DC) located at the transmission grid side works as a control center (CC). CC collects the real-time status information through polling the IEDs periodically. In this paper, generic substation event (GSE) messages are adopted with high speed peer-to-peer communication (any format of data is grouped into a data set and transmitted within a time period of 4 milliseconds). A set of configurations for IEDs are created respectively in CC for fault identification and analysis, which are called event tables, e.g. CB event table and relay event table. Each record in the event table has an element number corresponding to the monitored IEDs in the network [12]. A CB event table is shown in Fig.3, which is encoded in a binary way (1 means closed and 0 means open). Through retrieving the related event tables and checking the real-time measurements, the topology and status of the network can be confirmed. The subsequent decisions will be defined and executed. The protection settings of the relays for different states are calculated and stored offline in the settings table (action table).

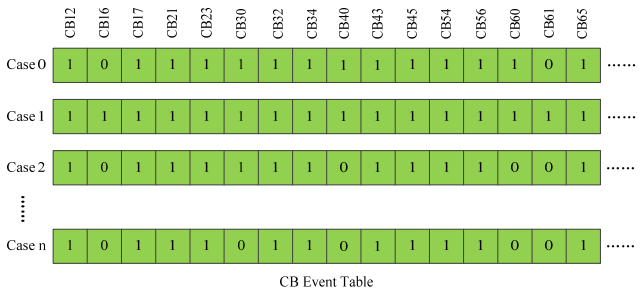

Fig. 3. Configuration of the CB event table.

The protection and control architecture is given in Fig.4. The remote communicate represents the information exchange with the utility. The open connectivity unified architecture (OPC UA) can be adopted as a middleware to communicate with external field, which is an industrial M2M communication protocol for interoperability. CC is the data concentrator located at the transmission grid side, monitoring and controlling the microgrid. The communication channel is the communication network between CC and on-field IEDs. The on-field devices normally contain the relays, CBs and measuring units. It is working as a part of SCADA in the whole distribution network.

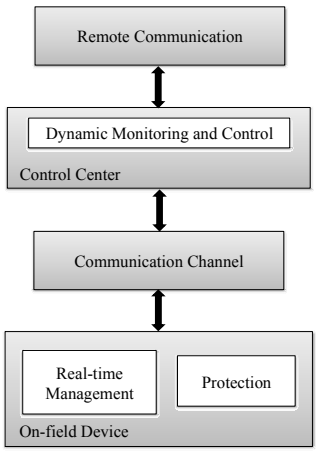

Fig. 4. Monitoring and control architecture.

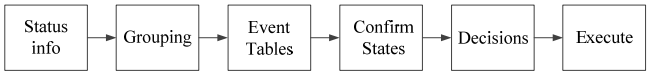

Fig. 5. Online monitoring and control algorithm with event table retrievals.

Fig.5 gives the online monitoring and control algorithm with event table retrievals in microgrid. The monitoring and control system is running online. The polling process can run periodically or triggered by an event (relay tripping, CB action and disturbance). Real-time status information is collected from different IEDs and grouped based on the trigger time. The objective of this action is to facilitate the retrieval of the events and group the information related to the same network events. Automatic analysis is followed to confirm the network status. Then, decisions are adopted according to the pre-settings in CC or the remote control from the utility. Finally, the decision is executed and recorded with exact time.

The short circuit events are simulated and the corresponding measurements are exported to Excel with DIgSILENT PowerFactory, while the analysis process is performed in MATLAB.

IV. DISTANCE PROTECTION

The main objection of distance protection is to calculate the impedance at the fundamental frequency between the fault point and the relay location. The impedance is calculated from the measuring voltage and current at the relay point. According to the calculated impedance, the fault is identified whether within the protection zone.

The measuring impedance Z_m is calculated from the measuring voltage $\dot{U}_m$ and current $\dot{I}_m$ at the relay point, which is shown in equation (1).

$$Z_m = \frac{\dot{U}_m}{\dot{I}_m} \tag{1}$$

Mho-based characteristic is adopted in this test, which is a basic element in the industrial distance relay. Each protection zone of the relay has a circular characteristic which is shown in Fig.6. Through the amplitude comparison between Z_m and Z_{set}, the relay decides whether trip the breaker or not. If $Z_m<Z_{set}$, it means the fault within the protection zone. On the contrary, the fault is out of the protection zone on the condition that $Z_m>Z_{set}$.

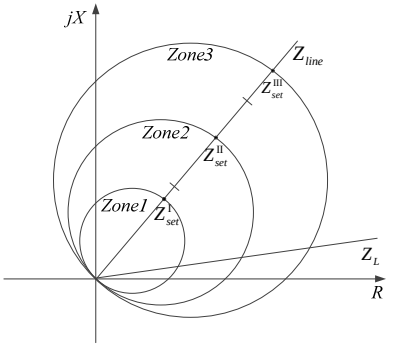

Fig. 6. Mho-based characteristics of distance relay.

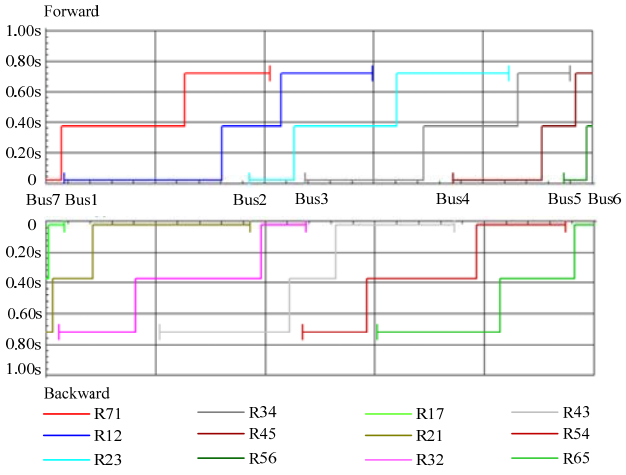

Fig. 7. The time-distance diagram of protection settings.

As shown in Fig.6, there are 3 protection zones for forward faults. Z_{set}^{I} is applied to Zone 1 protection. Z_{set}^{II} is applied to Zone 2 which provides protection for the rest of the protected line not covered by Zone1 and backup protection for the remote end bus. Z_{set}^{III} is applied to Zone 3 which provides remote back-up protection for adjacent lines. As a rule of thumb, Zone 1 covers 80%-85% of the protected line, Zone 2 covers 100% of the protected line plus 50% of the next line, Zone 3 covers 100% of both the protected line and the next line, plus 25%-50% of the third line. Here we define the constant time delay T_D^{II} =0.35s and T_D^{III} =0.7s for Zone 2 and Zone 3, respectively. Through the calculation and test, the final time-distance diagram of protection settings for normal operation is given in Fig.7.

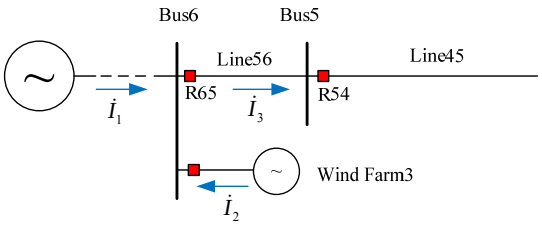

Fig. 8. The infeed current effect in the new topology.

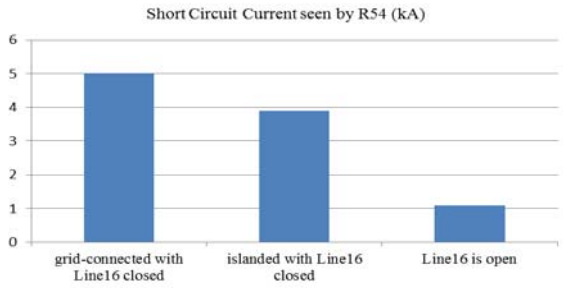

Fig. 9. Short circuit current on Line45 under different operation modes.

However, the topology reconfiguration of the microgrid should be considered further when Line16 is closed. The transmission grid and CHP plant may begin to affect the fault current on the backward relays with the infeed current, whose short circuit capacity can not be ignored compared to the wind farms. Here we take R65 and R54 as an example to explain the infeed current effect. Fig.8 gives the infeed current $\dot{I}_1$ in the new topology (Line16 is closed). $\dot{I}_1$ shortens the apparent impendence according to equation(1). The short circuit current seen by R54 is given in Fig.9. The short circuit current for grid-connected mode with Line16 closed is almost five times of the short circuit current when Line16 is open. To enhance the reliability and selectivity, the settings of backward relays should change the settings based on the current microgrid network.

The setting groups of the relays for different operation modes are all calculated and then restored by themselves. As soon as the new topology is detected in CC, it activates the related pre-settings recorded in the relays by telecommunication. Through the reconfiguration, the system operates in a new reliable operating mode.

V. CASE STUDY

According to the Danish grid code, WTG in the wind farms should withstand faults for at least 100ms. This is because the disconnection would bring additional stress on the already troubled system. The low voltage ride through (LVRT) capability for WTGs in the test is shown in Fig.10. The grey region represents the WTGs disconnected to the grid. It is designed to disconnect the WTGs when the voltage falls below 5% for more than 150ms [4]. The protection functions with associated operation settings and function time of the wind farms must be according to Table IV.

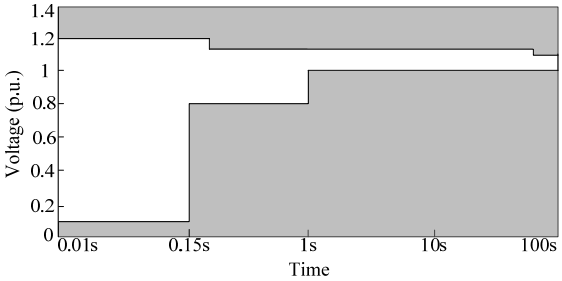

Fig. 10. Protection settings of WTGs.

TABLE IV. Requirements for the Wind Power Plants

Protective Function	Symbol	Setting	Function time
Overvoltage (step 3)	U>>>	1.2 U_n	5…200ms
Overvoltage (step 2)	U>>	1.1 U_n	200ms
Overvoltage (step 1)	U>	1.06 U_n	60s
Undervoltage	U<	0.9U_n	10…60s
Overfrequency	f>	52Hz	200ms
Underfrequency	f<	47Hz	200ms

The tests are simulated in DIgSILENT PowerFactory. The pickup time of the distance relay is 20ms and the circuit fault clearing time of the breaker is 60ms. Fig.11 gives the actual states of circuit breaker CB45 and CB54, when a fault occurs on the middle of Line45 at 0ms. In the simulation, CB=1 if the corresponding CB is closed and 0 if it is open. Fig.12 gives the corresponding fault currents seen by the relays.

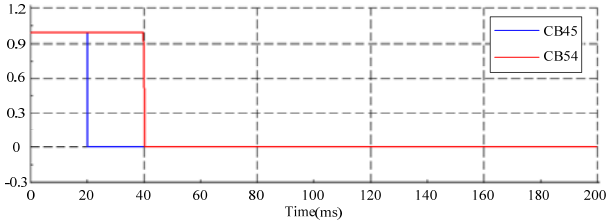

Fig. 11. States of CBs with normal distance protection.

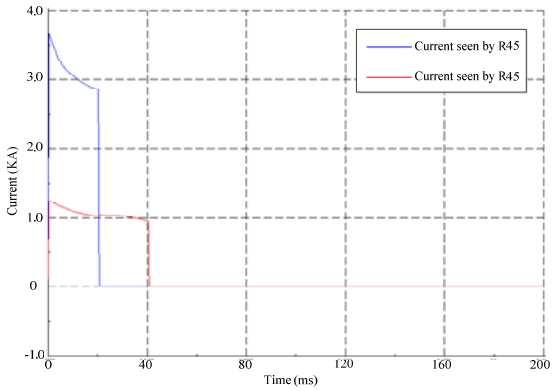

Fig. 12. Fault current in Line45 with normal distance protection.

From Fig.11 and Fig.12, we can find that R54 trips slower than R45. At the same time, the fault current seen by the forward relay R45 is much greater than the backward relay R54. This is mainly because there is only Wind Farm 3 supporting the backward fault current, whose short circuit capacity is much lower than CHP and the transmission grid. Therefore, the selectivity and sensitivity of the relays on Line45 and Line56 may be reduced due to the various operation modes.

Considering the effect of the intermittence of RE and the high impedance faults, permissive under-reach transfer tripping scheme (PUP Z2 scheme) is adopted to accelerate tripping the relays on the weak line. The tripping criterion is that the relay must detect the fault by Zone 2 before the remote end relay sends tripping signal. There is a telecommunication link among R45, R54, R56 and R65. The communication configuration is shown in Fig.13. Dual-redundant channels (CH1 and CH2) can be used to ensure the reliability. Automatic re-routing of signals is carried out in the event of a communication channel failure. The electrical variables monitored by each relay are transmitted and shared through CH1 and CH2. During the operation, if one of them detects a fault, the relay sends a tripping signal to the opposite relay on the same line segment e.g. the transfer tripping function between R45 and R54.

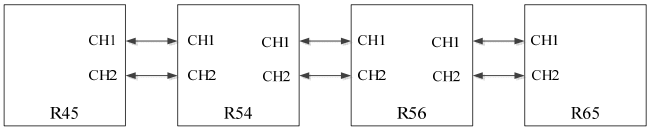

Fig. 13. Communication configuration of relays on line45 and line56.

At the beginning of Line45 (5% of the line segment), a three phase fault with 0.1Ω fault resistance is simulated at 0ms. Fig.10 shows the actual states of CB45 and CB54 with conventional distance protection. Since the fault occurs at the beginning of the line segment, R45 detects it very fast and trips at 20ms. For R54, however, the fault is out of the protection region of Zone 1 since it can only detect 85% to 90% of the line45 at most. Though Zone 2 detects this fault, there is a definite time delay (350ms) that needs to wait. At the same time, the WTGs in wind farm 3 are also facing the fault and providing the fault current for the backward relays. Unfortunately, according to the LVRT profile, the WTGs are tripped out at 150ms, which is shown in the Fig.14. The fault can not be cleared anymore without the backward fault current support. At the same time, there is a black out for Load5 which is an important load in the microgrid.

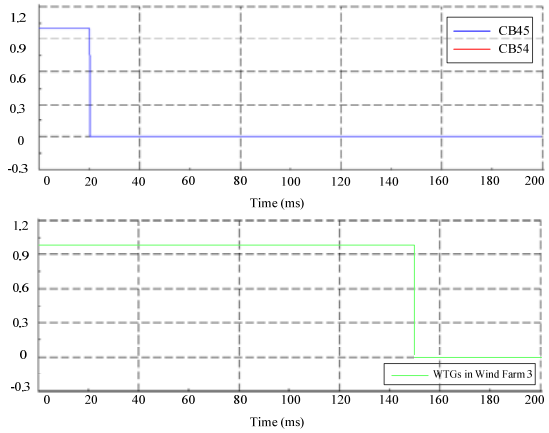

Fig. 14. States of CBs with normal distance protection.

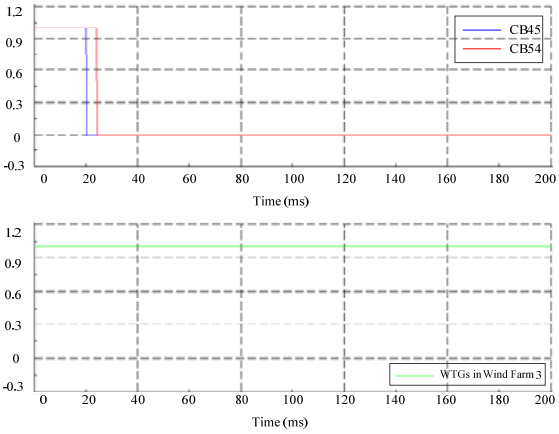

Fig. 15. States of CBs with adopting PUP Z2.

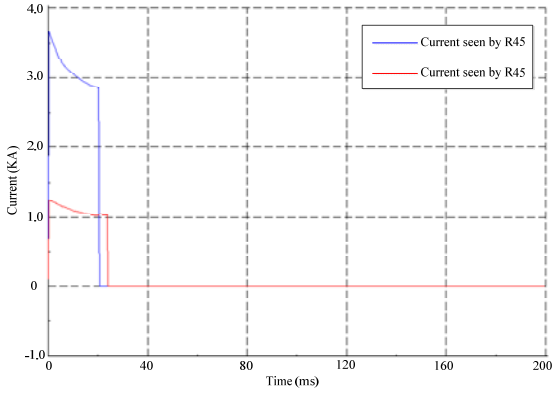

Fig. 16. Fault current in Line45 with adopting PUP Z2.

The states of CBs with the proposed distance protection are given in Fig.15. In the case of fault, R45 trips at 20ms and sends a tripping signal to the opposite relay R54 at the same time. After 4ms time delay (a constant communication delay time is assumed 4ms in this paper), R54 receives the tripping

signal. Since Zone 2 of R54 detects the fault before it receives the tripping signal from R45, which meets the PUP Z2 tripping criterion, R54 trips immediately. The WTGs in wind farm 3 keeps connecting to the grid for the fast fault clearing. The fault current with PUP Z2 scheme is given in Fig.16.

After the relays trip the fault, both relays send the real-time information to CC and trigger a fault event. CC confirms the state through retrieval and then recognizes the fault event based on the pre-settings. To ensure the reliability of power supply for Bus5 and Bus6, CC sends signals to close R16 and R61 after certain interval. The issue of synchronization should also be focused on for the connection between Bus6 and Bus1. It is beyond the scope of this paper, due to the space restriction. Here we assume the microgrid succeed in completing the reconfiguration. Then the settings for each backward relay (R65 and R54) are upgraded based on the new configuration, which are explained in Section IV. Meanwhile, the PUP Z2 scheme for Line56 is replaced by direct under-reach transfer tripping scheme, which trips directly once the relay receives the tripping signal from the opposite relay. The new scheme does not require Zone 2 detect the fault beforehand, which is different with PUP Z2. Fig.17 shows the new network of the microgrid after the reconfiguration.

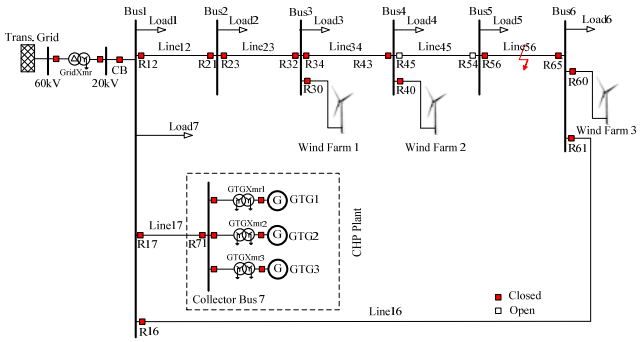

Fig. 17. The new network of the microgrid after the reconfiguration.

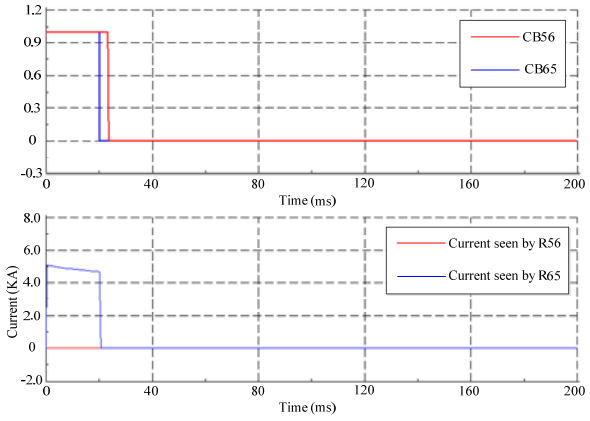

Fig. 18. The actual states of CBs and fault currents on Line56.

Another three phase fault with 0.1Ω fault resistance is simulated on the middle of Line56 at 0ms for the new configuration. We can find that there is no forward fault current support for R56 in Fig.17, certainly neither for Zone 2. Whereas, R56 still can trip the fault fast with the modified direct under-reach transfer tripping scheme. The actual states of CBs and fault currents on Line56 are given in Fig.18.

VI. CONCLUSION

For the increasing penetration of RE, a coordinative PMU-based adaptive distance protection is proposed for one microgrid network. Through retrieving the related event tables and checking the real-time measurements, the topology and status of the network can be confirmed in the data collector that located in the transmission grid side. The settings of each relay are calculated and recorded for different operation modes. Transfer tripping is adopted to accelerate the relay tripping for the weak power lines. The preferred protective response to a change will be modified based on the system conditions or requirements. Compared to the adaptive overcurrent protection and differential protection, this adaptive distance protection methodology has almost the same investment. However, it has better capability on monitoring and control of the whole system with high-resolution real-time measurement.

Reference:

[1] W. Mu and C. Zhe, "Distribution system protection with communication technologies," in *IECON 2010 - 36th Annual Conference on IEEE Industrial Electronics Society*, pp. 3328-3333, 2010.

[2] W. Hui, K. K. Li, and K. P. Wong, "An multi-agent approach to protection relay coordination with distributed generators in industrial power distribution system," in *Industry Applications Conference, 2005. Fourtieth IAS Annual Meeting. Conference Record of the 2005*, Vol. 2, pp. 830-836. 2005.

[3] Z. Q. Bo, "Adaptive non-communication protection for power lines BO scheme. II. The instant operation approach," *IEEE Trans. Power Delivery*, vol. 17, pp. 92-96, 2002.

[4] P. Mahat, C. Zhe, B. Bak-Jensen, and C. L. Bak, "A Simple Adaptive Overcurrent Protection of Distribution Systems With Distributed Generation," *IEEE Trans. Smart Grid*, vol. 2, pp. 428-437, 2011.

[5] A. H. Osman and O. P. Malik, "Transmission line distance protection based on wavelet transform," *IEEE Trans. Power Delivery*, vol. 19, pp. 515-523, 2004.

[6] J. Lorenc, A. Kwapisz, and K. Musierowicz, "Efficiency of admitance relays during faults with high fault resistance values in MV networks," in *Power Tech, 2005 IEEE Russia*, pp. 1-5, 2005.

[7] Z. Zhang and D. Chen, "An Adaptive Approach in Digital Distance Protection," *IEEE J. Power Engineering Review*, vol. 11, p. 44, 1991.

[8] W. D. Breingan, M. M. Chen, and T. F. Gallen, "The Laboratory Investigation of a Digital System for the Protection of Transmission Lines," *IEEE Trans. Power Apparatus and Systems*, vol. PAS-98, pp. 350-368, 1979.

[9] K. Yabe, "Power differential method for discrimination between fault and magnetizing inrush current in transformers," *IEEE Trans. Power Delivery*, vol. 12, pp. 1109-1118, 1997.

[10] M. M. Eissa and O. P. Malik, "A new digital directional transverse differential current protection technique," *IEEE Trans. Power Delivery,*, vol. 11, pp. 1285-1291, 1996.

[11] A. G. Phadke, "Synchronized phasor measurements-a historical overview," in *Transmission and Distribution Conference and Exhibition 2002: Asia Pacific. IEEE/PES*, vol.1, pp. 476-479.

[12] Oudalov A, Fidigatti A. "Adaptive network protection in microgrids". *International J. Distributed Energy Resources*, pp. 201-226, 2009.

[13] Liu C, Rather Z H, Chen Z, et al. "Multi-agent system based adaptive protection for dispersed generation integrated distribution systems". *IEEE J. Smart Grid and Clean Energy*, vol. 2, pp. 406-412, October 2013.